Wireless (Power Transfer) Transmission of Electrical Energy (Electricity) Intended for Consumer Purposes up to 50 W

Marek PIRI, Pavol SPANIK, Michal FRIVALDSKY, Anna KONDELOVA

Department of Mechatronics and Electronics, Faculty of Electrical Engineering, University of Zilina,
Univerzitna 8215/1, 01026 Zilina, Slovak Republic

marek.piri@fel.uniza.sk, pavol.spanik@fel.uniza.sk, michal.frivaldsky@fel.uniza.sk, anna.kondelova@fel.uniza.sk

Abstract. *This project deals with Power Semiconductor Systems PSS for wireless transmission of electricity to the power of 50 W with regard to the distance and transmission efficiency. We decided to use electromagnetic resonance for electrical energy transmission. For experimental verification, we have wound two coils of identical dimensions. At a given power transmission solutions, we obtain the highest efficiency $\eta = 70$ % at a distance of 5 cm, where the transmitted power was 48 W.*

Keywords

Coil, frequency, resonant, wireless power transfer.

1. Introduction

Wireless transmission of electricity is a vision that circulates in the minds of inventors for over 100 years. Discovering of magnetic resonance opened the way for solving the problem of efficiency of electricity transmission in the near field. Thanks to this phenomenon, it is possible to transfer a high power capacity at high efficiency. The result is a prospective solution for many applications such as consumer electronics, automotive systems, medical equipment and many more. The aim of the paper is to design a topology of PSS for wireless transmission of electricity with the power up to 50 W with regard to the distance and transmission efficiency. Analysis of currents of main circuit for the wireless transfer system, has to help successful implementation of the task. The choice of the optimal design to achieve the specified parameters, the simulation of the designed system and its structure is based on this analysis. The article consists of several parts. The first is devoted to analysis and the current state of system solutions for the wireless transmission of electricity. The second part of the article describes the design of the main circuit for the wireless transmission. In the third part of the paper the simulation model is provided that is based on an earlier proposal and describes the behavior of the proposed system. The experimental verification of the designed solution the aim of which is an efficient transmission of electricity from the source to the load without the use of wires is performed in the fourth part of this work.

2. Applied Type of Coupling and its Analysis

When the mutual inductance of two coils is low, the receiver coil induces the low voltage with a low efficiency. According to Eq. (1) we can see that the low M value may be compensated by an increase in the angular frequency ω, or by an increase in the I_1 amplitude of the transmitting coil.

$$u_p(t) = \frac{d\phi}{dt} = M\frac{di_1(t)}{dt} = M\omega I_1 \cdot \cos(\omega t). \qquad (1)$$

There are two types of power systems for wireless transmission-direct and indirect power supply (Fig. 1).

At indirect power supply, transmitting and receiving coil is separated from the source and load to achieve higher quality factor Q at the transmitting and receiving part, whereby it is possible to achieve greater transmission distance. Coils L_1 and L_2 serve as binding coils, which transform the impedance of source and load. Reaching the higher quality factor Q can increase
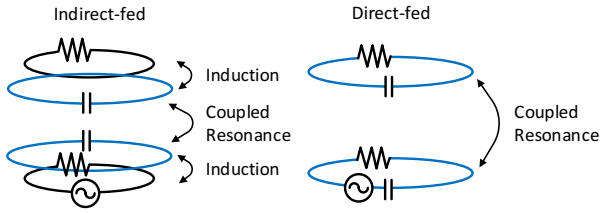
Fig. 1: Wireless transmission in direct and indirect power supply.

transmitted distance. However, the systems are more sensitive to the choice of parameters such as the inductance and the resonance frequency. Direct type of power supply indicates from the title that the source is directly connected to the transmitter section. A choice of this type of power supply is more suitable for practical applications because of the simplicity of the design, customization options, control and low cost. Its disadvantage is the reduction of the quality factor Q [1], [2], [3], [4].

3. Design of the System of Selected Transmission Method

The usage of the resonant circuit in the receiver and transmitter allows transmitting of the highest transmitted capacity at the highest possible distance. For this type of transmission, it is important to design a low-loss coils and pairing circuits. Fulfilment of the given conditions in the design allows achievement of the best transmission parameters. Topology design is based on the principle diagram for the resonant wireless system for electricity transmitting (Fig. 2).
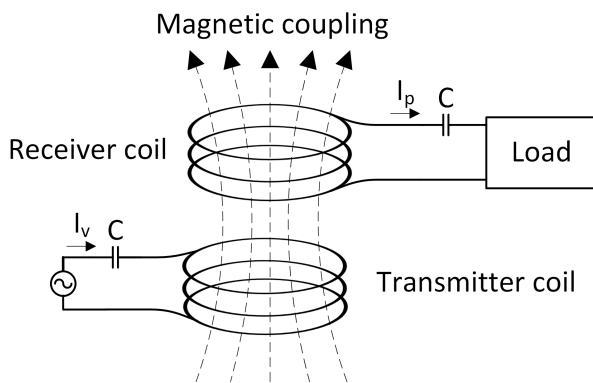

Fig. 2: Principles schematic of the resonant wireless system.

DC voltage source supplies power amplifier (DC/AC), which produces rectangular voltage waveform. This voltage produces an alternating magnetic field in a transmission resonant circuit. Receiving

resonant circuit is tuned to the same resonant frequency as the source frequency. Magnetic energy induces a sinusoidal voltage at the receiving side. The AC voltage is then rectified in a diode rectifier and DC voltage is led to the load [5], [6]. Based on the predicted performance, we set other parameters.

Tab. 1: Other parameters.

U_{in}	100 V
P_{out}	50 W
U_{out}	20 V
I_{out}	2.5 A
R_L	8 Ω
f_{SW}	293 kHz

4. The Coil Design

The coil design is one of the most important factors in the design of a system for wireless transmission. Important parameters such as quality factor Q and mutual inductance that determine the maximum transmission efficiency, maximum transmission distance and also the transmission capacity depends on the parameters of transmitter/receiver coil. Inductance calculation normally begins on the so-called pure inductor, when it is assumed that the solenoid coil is formed of infinitely thin wire without gaps between conductors (turns of wire are electrically isolated). The main characteristic of this coil is that at low frequencies it radiates uniform magnetic field over the whole length. As far as these conditions are met, we can write:

$$L_s = \frac{\mu \pi D^2 N^2}{4h}, \qquad (2)$$

where μ is the relative permeability of vacuum, D is the diameter of the coil, N is the number of turns and h is the length of the coil Fig. 3. Pure inductor is a theoretical model, but we can use it after a small modification. The modification can be divided into two parts, frequency-dependent and frequency-independent.
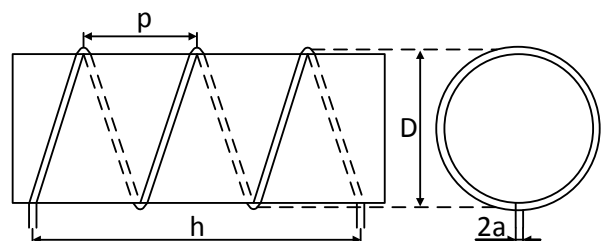

Fig. 3: Layout and dimensions of coil.

At frequency independent modification, coefficient k_L describes the irregularity of the field and is expressed in Eq. (3) [7], [8], [9], [10], [11].

$$k_L = \frac{2h}{D} \cdot \left(\frac{\left(\ln\left(\frac{4D}{h}\right) - \frac{1}{2} \right) \cdot \left(1 + 0.393901 \cdot \left(\frac{h}{D}\right) + 0.017108 \cdot \left(\frac{h}{D}\right)^4 \right)}{1 + 0.258952 \cdot \left(\frac{h}{D}\right)^2} \right.$$
$$\left. + 0.093842 \cdot \left(\frac{h}{D}\right)^2 + 0.002029 \cdot \left(\frac{h}{D}\right)^4 - 0.000801 \cdot \left(\frac{h}{D}\right)^6 \right). \tag{3}$$

Then, an equation for inductance L_S can be written according to Eq. (2).

$$L_S = \frac{\mu \pi D^2 N^2}{4h}. \tag{4}$$

For real coils, it is needed to include the coefficient k_S, which takes into account circular conductor cross-section and the coefficient k_m for the mutual inductance between the turns.

$$k_s = \frac{3}{2} - \ln\left(\frac{p}{a}\right). \tag{5}$$

$$k_m = \ln(2\pi) - \frac{3}{2} - \frac{\ln(N)}{6N} - \frac{0.33084236}{N}$$
$$- \frac{1}{120N^3} + \frac{1}{504N^5} - \frac{0.0011923}{N^7} + \frac{0.0005068}{N^9}. \tag{6}$$

$$L = L_s - \frac{\mu N D}{2(k_s + k_m)}. \tag{7}$$

Two other parasitic elements: the skin effect and proximity effect should be taken into consideration at high frequencies, respectively at frequency dependent modulation. The so-called internal induction, which is an imaginary contra equivalent of the skin effect, rapidly decreases with increasing frequency and is proportional to the length of the conductor, affects the calculation of the induction coil. The effect of the internal inductance, however, can be used only for short coils.

$$L_i = \frac{\mu_0 \delta_i \left(1 - e^{\left\{ -\left[\frac{a}{2\delta_i} \right]^{3,8} \right\}} \right)^{\frac{1}{3,8}}}{4\pi a} (1 - y)\, l, \tag{8}$$

where μ_0 is the permeability of vacuum, δ_i - depth of penetration, a - the radius of the conductor, l - total length of the coil conductor.

$$y = \frac{0.0239}{\left(1 + 1.67\left(z^{0.036} - z^{-0.72} \right)^2 \right)^4}. \tag{9}$$

$$z = \frac{a}{2.552\delta_i}. \tag{10}$$

$$l = \sqrt{(\pi N D)^2 + h^2}. \tag{11}$$

The final formula to calculate the inductance of coil with all corrections is as follows:

$$L = L_s - \frac{\mu N D}{2}(k_s + k_m) + L_i, \tag{12}$$

where L_S is inductance of the pure inductor, μ_0 is vacuum permeability, n is number of turns, k_s, k_m are correction factors and L_i is internal coil inductance. So called Litzwire-high frequency cable is used to suppress the negative effects of frequency dependent part of resistance of a coil conductor in the high frequency systems. Its task is the suppression of skin effect and proximity effect [12]. High-frequency cable is made up of tangled thin insulated wires, the recommended diameter of which is:

$$d \leq 2\delta, \tag{13}$$

where d is the conductor diameter and δ it is the depth of penetration. Litzwire should be used only for frequencies from 50 kHz to 3 MHz. If the two coils have the same radius, the same number of turns and are held in the same axis, their mutual inductance can be determined:

$$M = \mu_0 \frac{D}{2} N^2 \int_0^\pi \frac{\cos x}{\sqrt{2(1 - \cos(x)) + \left(\frac{d}{D}\right)^2}} dx. \tag{14}$$

Based on established parameters and relationships, the parameters of the being designed coil are calculated according to Tab. 2.

Tab. 2: Calculated parameters of the designed coil.

Par.	Value	Unit	Describe
D	185	(mm)	Coil average
l	60	(mm)	Coil length
a	1.5	(mm)	Wire average
N	6	(-)	Numb. turns
f	300	(kHz)	Frequency used in design
p	10	(mm)	Pitch
Φ	1.06	(-)	Proximity factor
k_L	0.442	(-)	C. f. inequalities field
k_s	-1.34	(-)	C. f. self ind. Of round wire
k_m	0.233	(-)	C. f. mutual ind. Of round wire
l	3486	(mm)	Physical length of were
d_{min}	<0.36	(mm)	Recommended min. thickness cable wire
N_{LW}	32	(-)	Num. of cable for litz-wire
δ_l	120	(μm)	Penetration depth
L	9.34	(μH)	Inductance
R	0.062	(Ω)	Serial AC resistance
C	1020	(pF)	Parasitic capacitance
Q	174	(-)	Quality factor
f_{rez}	22.652	(MHz)	Self res. freq. of coil

For the calculation of the mutual inductance M the Eq. (12) was used and the results are shown in Tab. 3.

Tab. 3: Mutual inductance of two symmetrical coils.

Distance (cm)	5	10	15	20	25
M (μ)	3.44	1.465	0.726	0.398	0.237
k (-)	0.368	0.157	0.078	0.043	0.025

Where k is the coupling factor which is calculated by the following formula:

$$k = \frac{M}{\sqrt{L_1 L_2}}. \qquad (15)$$

5. Calculation of Parameters and Circuit Elements

For the analysis of topologies, it has been chosen a suitable test topology with series serial connection of the compensation capacitor, Fig. 4. Here the choice of topology determines the further calculations of elements and circuit parameters.
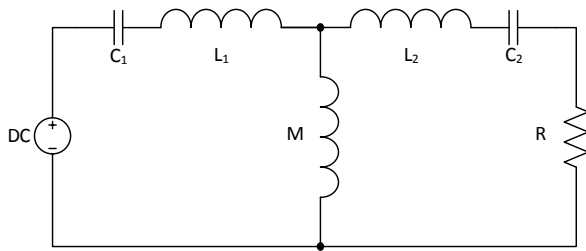
Fig. 4: Serial capacitive compensating of capacitor.

The following equation was used for the calculation of the transformation ratio:

$$n = A_V \frac{\frac{U_{in}}{2}}{U_{out}} = \frac{\frac{U_{in}}{2}}{U_{out}} |_{A_V=1} = 2.5. \qquad (16)$$

Transformation ratio between primary and secondary coil was chosen to 1 to simplify the design and the desired output voltage has been achieved with a frequency control [13]. Similarly, this solution is preferred in light of the coil structure and further design of the system. Value of compensation capacity C_2 of the secondary side is calculated from equation:

$$C_2 = \frac{1}{\omega_0^2 L_2} = 31.16 \text{ nF}. \qquad (17)$$

Next, the value of primary side compensation capacity C_1 was calculated:

$$C_1 = \frac{L_2 C_2}{L_1} = 31.16 \text{ nF}. \qquad (18)$$

Capacity values are rounded to the next higher production series C_1, C_2 = 33 nF. Next, the

efficiency for a given topology at a distance of 5 cm was calculated, where $M = 3.44$ μH.

$$\eta = \frac{R_L}{(R_L + R_2)\left(1 + \frac{R_1(R_2 + R_L)}{\omega^2 M^2}\right)}. \qquad (19)$$

Then, the quality factor Q of transmitter (primary side) and of the receiver (secondary side) may be calculated:

$$Q_1 = \frac{L_1 R_L}{\omega_0 M^2} = 3.43. \qquad (20)$$

$$Q_2 = \frac{\omega_0 L_2}{R_L} = 2.15. \qquad (21)$$

Calculated values are decisive, but their values are only theoretical. The main reason is that the calculation was provided only for the resistance of the coils. Wire resistance, capacitors resistance and influence of disturbing elements have been neglected.

6. Time Dependent Analysis

Mutual induction was calculated for five distances (Tab. 4) and used as a variable parameter. The simulations were solved for two cases. The first was the measurement of output voltage, current, and efficiency at a resonant frequency. The second simulation was aimed at changing the frequency and the achievement of constant output parameters $V_{out} = 20$ V and $I_{out} = 2.5$ A, in order to achieve the desired output power of 50 W. Voltage and current waveforms at individual components are displayed for one selected value of coils distance (5 cm).

Tab. 4: The simulation results for a constant frequency at $A_v = 1$ s.

Distance	Equivalent circuit			K_linear		
(cm)	U (V)	I (A)	η (%)	U (V)	I (A)	η (%)
5	42	4.84	80	46.7	5.5	83
10	33.6	3.95	56	34	4	56
15	27.8	3.26	26	30	3.5	26
20	19.5	2.35	10	18.5	2.1	9
25	12.8	1.42	3	10.8	1.25	3.5

The value of resonance frequency was 286 675 Hz. From the previous simulation and the voltage transmission characteristics, it is known that a voltage gain is equal to 1 then. However, the operation mode of switching transistors at this point is not ideal and the suitable operating mode of switching at zero voltage (ZVS) is above the resonant frequency.

For best results, the range from 286 kHz to 296 kHz was chosen, which is close to the resonant frequency and for the nine values the parametric simulation was
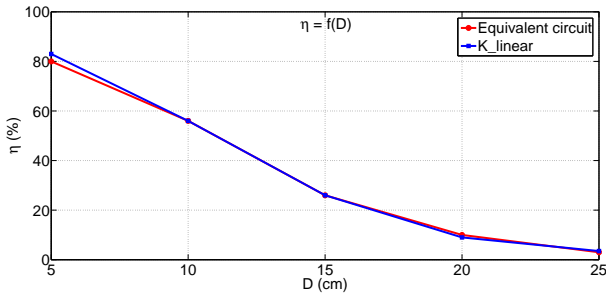
Fig. 5: Dependence of efficiency on the distance to the constant frequency.
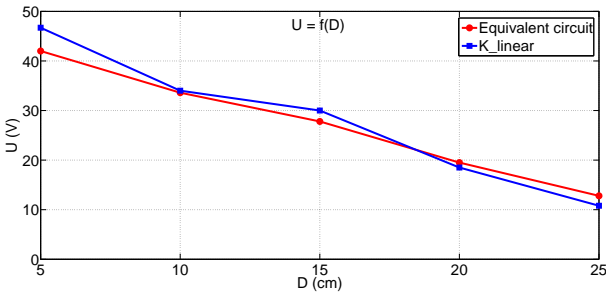

Fig. 6: Dependence of secondary voltage on the distance to the constant frequency.

performed from which the most suitable frequency was determined in terms of efficiency. It was 290 kHz. Maximum efficiency was 83 % for the simulation model using K_linear block. The difference between using a transformer equivalent circuit and K_linear block is minimal, so the results can be considered correct. The voltage and current waveforms at each component are displayed for 5 cm value.
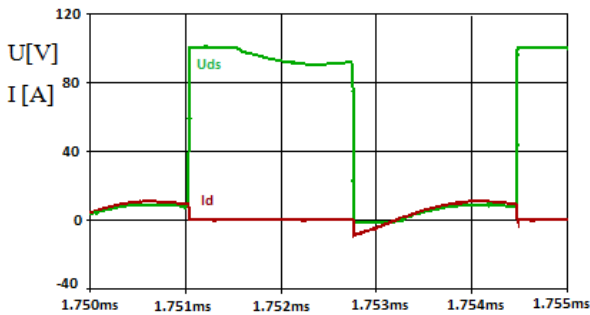

Fig. 7: The time waveforms of the voltage U_{ds} and current I_d of transistor T_1 for 5 cm.

Tab. 5: Simulation results for the constant U_{out} and I_{out}.

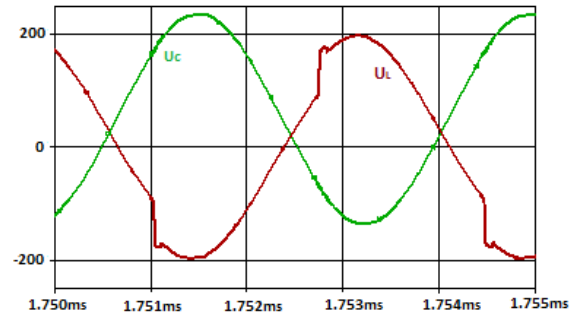|	ZVS		ZCS	
Distance (cm)	η (%)	f (Hz)	η (%)	f (Hz)
5	73	326250	30.5	196078
10	53	305510	26	229357
15	26	294117	11.5	251889
20	8.7	289885	5.2	265252
25	3	287356	2.5	277777

Fig. 8: The time waveforms of the voltage at resonant elements of transmitting side for 5 cm distance.
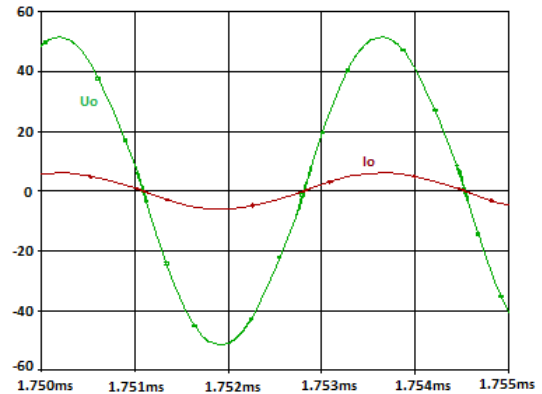

Fig. 9: The time waveforms of the voltage and current at the load without a rectifier bridge for 5 cm distance.
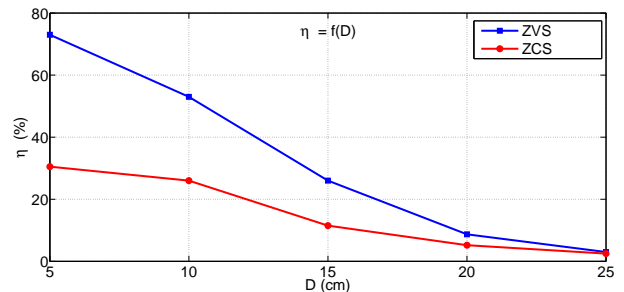

Fig. 10: Dependence of the effectiveness on the distance for constant U_{out} and I_{out}.
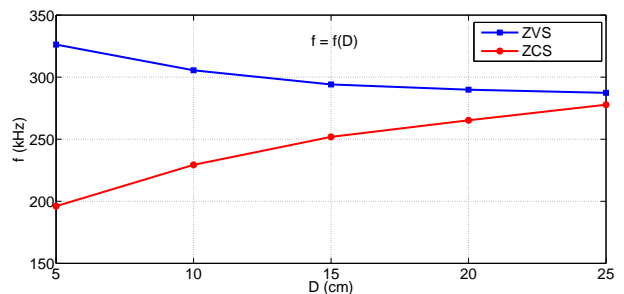

Fig. 11: Dependence of T_{ws} change on the distance for constant U_{out} and I_{out}.

As the transformation ratio of coils was 1:1, the change in the output voltage and current was ensured with the change in switching frequency. The Tab. 5 shows that zero voltage switching (ZVS) is more preferred in terms of efficiency than switching at zero current. From the measured values it is confirmed that the system is more sensitive to changes of frequency at a longer distance. The chart of frequency dependence on the distance (Fig. 10) shows that with the increasing distance it is necessary to approach to the resonance frequency to obtain a sufficient gain.

7. Experimental Verification on Physical Model

We have created a physical model to verify the correctness of the designed solutions on the basis of theoretical analysis and simulation analysis in the previous chapters. Design of physical model is based on several parts: on the choice of topology from theoretical documents, on the type of circuit power supply, on choice of switching transistors, suitable capacitors, on construction of transmitter and receiver coils. The whole system is divided according to the block diagram Fig. 7, which was created in the theoretical design of the system. A half bridge connection of transistors is used as a DC/AC inverter similarly to simulation model. For this purpose, the wiring on the universal board for a half bridge circuit was used. Transistors FDPF17N60NT are used for switching. Their selection has been made on the basis of simulation analysis, from which we see that the transistors current I_d at lower distances is 8 A and it is growing with increasing distance. The transistors are suitable for the maximum allowable voltage.

Tab. 6: Basic parameters.

I_d	17 A
U_{ds}	600 V
$R_{ds}(\text{on})$	340 mΩ

The physical model was powered by a DC system source Agilent N5771A. During the design, it was considered a production series of capacitors MKP or MKT having low ESR values. As in the simulations, in the experimental physical model 33 nF value was used for the transmitter and the receiver side too. To reduce the voltage and current load, the capacitor of transmitting (primary) side was made up of series parallel capacitors Fig. 12.

For the proposed system, two identical coils were made, the dimensions of which can be found in Section 5. The coil design. Wire of coil is formed of 32 tangled thin insulated wires with a diameter of 0.18 mm. A non-conductive material (extruded polystyrene) was used as a frame of coil. The calculated

inductance value in the design of coil at the designed frequency of 100 kHz was $L = 9.34$ μH and its quality factor $Q = 94.7$. The RLC meter was used to verify the design. Following parameters were measured at the 100 kHz. $L_1 = 9.57$ μH, $Q_1 = 69$ and $L_2 = 9.12$ μH, $Q_2 = 59$. The resulting values are influenced mainly by certain construction elements such as cable lengths, the tendency of individual turns, and by the fact that the resulting coil is not a perfect circle. However, the goal was achieved and the difference between the calculated and measured inductance is within a standard.

Fig. 12: View of the series-parallel connection of capacitors - 33 nF.
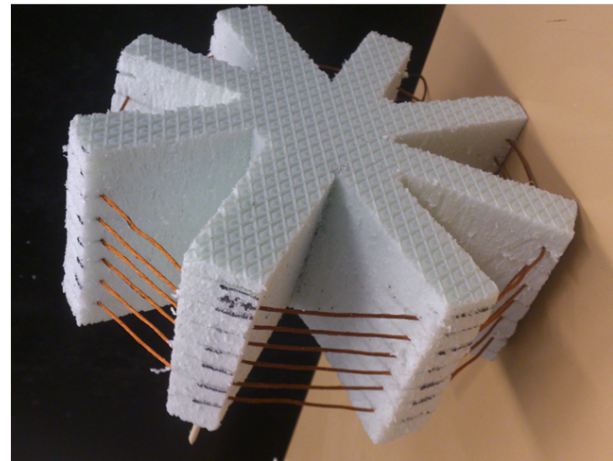

Fig. 13: View on a designed coil.

The output rectifier was connected as bridge rectifier. It was designed from Schottky diodes STPS10H100CT due to the high working frequencies. Used load had only resistive character. It was built of four non-inductive resistors connected in parallel and its resulting value was 8.25 Ω.

8. Measurements on Physical Model

Created physical model for the wireless transmission of electrical energy has been subjected to measurement. Time courses were recorded on an oscilloscope Tektronix TDS 3024B that allows the storage of scanned waveform in the data file. The current probe Tektronix TCP A306 and the differential voltage probe HZ100 HAMEG were applied for taking the time waveforms of voltage and current on the load. The resulting waveforms were processed in a spreadsheet program and graphically displayed. The resulting measured values of voltage and current on the load were truncated for one period for graphical representation. The resulting graph was interpolated by trend line formed with the polynomial of the sixth degree because of variability and large amounts of data. The equation of the trend line is shown in the Fig. 14 where y_U is an equation for voltage and y_I is an equation for current. For each measurement input, output power and efficiency were then calculated. An example calculation is measuring for distance 5 cm between the coils.
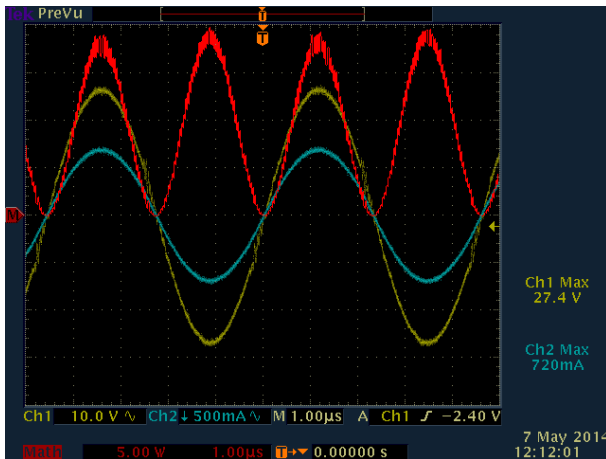

Fig. 14: Dependence of output voltage and output current for a distance of 5 cm at constant switching frequency.

Tab. 7: Measurement at a distance of 5 cm.

U_{in} (V)	P_{in} (W)	I_M (A)	φ ()	I_{in} (A)	U_M (V)	T (μs)	η ()
99.9	67.93	3.43	0	0.68	27.92	3.4388	

$$P_{out} = \frac{1}{T} \int_0^T U_M \sin(\omega t) \cdot I_m \sin(\omega t + \varphi)\, dt. \quad (22)$$

$$P_{out} = \frac{1}{3.4388 \cdot 10^{-6}}$$

$$\cdot \int_0^T 27.92 \cdot \sin\left(2\pi \cdot 290799 \cdot t\right) \quad (23)$$

$$\cdot 3.43 \cdot \sin\left(2\pi \cdot 290799 \cdot t\right) = 4.$$

$$\eta = \frac{P_{out}}{P_{in}} = \frac{47.88}{67.93} = 0.705. \quad (24)$$

Tab. 8: Measurement at a distance of 10 - 20 cm.

Measurement at a distance of 10 cm							
U_{in} (V)	P_{in} (W)	I_M (A)	φ ()	I_{in} (A)	U_M (V)	T (μs)	η ()
99.9	63.94	1.83	13.49	0.64	14.74	3.43	0.21
Measurement at a distance of 15 cm							
U_{in} (V)	P_{in} (W)	I_M (A)	φ ()	I_{in} (A)	U_M (V)	T (μs)	η ()
99.9	62.94	1.05	4.22	0.63	8.04	3.43	0.08
Measurement at a distance of 20 cm							
U_{in} (V)	P_{in} (W)	I_M (A)	φ ()	I_{in} (A)	U_M (V)	T (μs)	η ()
99.9	62.94	0.63	1.51	0.63	4.8	3.43	0.02

9. Conclusions

Design of systems for wireless transmission is currently promising area of research and development, in respect of the wide range of applications where it is possible to use this technology. For the design and construction today there is still no strict procedure for achieving the desired resultant parameters, therefore solving of the given issue is not uniform, however, it is based on the phenomenon of magnetic resonance.

In this paper we have set a target to design the PSS topology for wireless transmission of electricity with power up to 50 W. In the process solutions, we divided the work into three parts - theoretical, theoretical-practical and practical. In them, we focused on important individual design analysis. In the theoretical part we went into the history of wireless transmission and we described the various options of wireless transmission of electricity. From this initial theoretical analysis, we decided for transmission by means of electromagnetic resonance. Explanation of important factors that enter into this type of transmission and influence it was a continuation of theoretical analysis.

Theoretical-practical part was used for summarizing of possible solutions and for choosing of the appropriate system topology for wireless transmission. We have created a block diagram of the circuit and in the same part we have made the design of system and design of the coil. In the practical part we have created the simulation model first, which we used to predict the behavior of the designed system. It also gave us the

results that we then compared with measurements on a physical model.

We have spooled two coils with identical dimensions for the experimental verification of the system. Compared to the theoretical calculation, deviation of their inductance was 3 %, but the quality factor was lower than 38 %. We have then created an experimental wiring according to the simulation model and we performed measurements for four distances. The highest achieved efficiency of 70 % was for 5 cm distance and the transmitted power was 48 W. We have met the main aim of this paper We have designed PSS topology for wireless transmission of electric energy with power up to 50 W and we have experimentally verified the solution's correctness. Based on the knowledge obtained during paper solutions we have written some recommendations for further development of the system design for wireless transmission of electric energy.

Acknowledgment

References

[1] PANKRAC, V. The Algorithm for Calculation of the Self and Mutual Inductance of Thin-Walled Air Coils of General Shape With Parallel Axes. *IEEE Transactions on Magnetics.* 2012, vol. 48, iss. 5, pp. 1875–1889. ISSN 0018-9464. DOI: 10.1109/TMAG.2011.2177854.

[2] WEISSTEIN, E. W. Elliptic Integral of the Third Kind. In: *MathWorld–A Wolfram Web Resource* [online]. 2015. Available at: http://mathworld.wolfram.com/EllipticIntegraloftheThirdKind.html.

[3] GLAD, M. Design of photovoltaic solar cell model for stand-alone renewable system. In: *ELEKTRO.* Rajecke Teplice: IEEE, 2014, pp. 285–288. ISBN 978-1-4799-3720-2. DOI: 10.1109/ELEKTRO.2014.6848903.

[4] TIRPAK, A. *Elektromagnetizmus.* 1st ed. Bratislava: Polygrafia SAV, 1999. ISBN 80-88780-26-8.

[5] PAVLANIN, R., B. DOBRUCKY and P. SPANIK. Investigation of compensation effect of shunt active power filter working under the non-sinusoidal voltage conditions. *International Review of Electrical Engineering.* 2009, vol. 4, iss. 5, pp. 785–791. ISSN 1827-6660.

[6] Developement Board EPC 9003C Quick Start Guide. In: *EPC: Efficient Power Conversion* [online]. 2011. Available at: http://epc-co.com/epc/documents/guides/EPC9003_qsg.pdf.

[7] KINDL, V. Key construction aspects of resonant wireless low power transfer system. In: *ELEKTRO.* Rajecke Teplice: IEEE, 2014, pp. 303–306. ISBN 978-1-4799-3720-2. DOI: 10.1109/ELEKTRO.2014.6848907.

[8] KACSOR, G., P. SPANIK, J. DUDRIK, M. Luft and E. Szychta. Principles of Operation of Three-level Phase Shift Controlled Converter. *Elektronika IR Elektrotechnika.* 2008, vol. 82, no. 2, pp. 69–74. ISSN 2029-5731. Available at: http://www.eejournal.ktu.lt/index.php/elt/article/view/11058/5803.

[9] BRANDSTETTER, P., P. CHLEBIS, P. PALACKY and O. SKUTA. Application of RBF network in rotor time constant adaptation. *Elektronika IR Elektrotechnika.* 2011, vol. 113, no. 7, pp. 206–212. ISSN 1335-3632.

[10] GRMAN, L., M. HRASKO, J. KUCHTA and J. BUDAY. Single phase PWM rectifier in traction application. *Journal of Electrical Engineering.* 2011, vol. 62, iss. 4, pp. 206–212. ISSN 1335-3632. DOI: 10.2478/v10187-011-0033-z.

[11] FERKOVA, Z., M. FRANKO, J. KUCHTA and P. RAFAJDUS. Electromagnetic design of Ironless Permanent Magnet Synchronous Linear Motor. In: *International Power Electronics, Electrical Drives, Automation and Motion.* Ischia: IEEE, 2008, pp. 721–726. ISBN 978-1-4244-1663-9. DOI: 10.1109/SPEEDHAM.2008.4581085.

[12] KOVACOVA, I. and D. KOVAC. Inductive Coupling of Power Converter's-EMC. *Acta Polytechnica Hungarica.* 2009, vol. 6, no. 2, pp. 1–53. ISSN 1785-8860.

[13] RADVAN, R., B. DOBRUCKY, M. FRIVALDSKY and P. RAFAJDUS. Modelling and Design of HF 200 kHz Transformers for Hard- and Soft-Switching Application. *Elektronika IR Elektrotechnika.* 2011, vol. 110, no. 4, pp. 7–12. ISSN 2029-5731. DOI: 10.5755/j01.eee.110.4.276.

About Authors

Marek PIRI was born in Sahy, Slovak Republic. He graduated study at University of Zilina (2006).

Nowadays study at Ph.D. grade at Department of Mechatronics and Electronics at University of Zilina. He is interesting in the field of power electronics-switch mode power supplies, simulations, design of power supplies.

Pavol SPANIK graduated at University of Transport and Communications in Zilina (1978), in the field of Electrical traction and energetics in transport. Nowadays works at Department of Mechatronics and Electronics of Faculty of Electrotechnical Engineering at University of Zilina. He is interested in the field of power electronics, mechatronics and control systems.

Michal FRIVALDSKY was born in Stara Lubovna, Slovak Republic. He graduated study at University of Zilina (2006). He finished his Ph.D. Study in the field of

power electronics at the University of Zilina (2009) and became assoc. prof. in 2014. Nowadays he works at the Department of Mechatronics and electronics, Faculty of Electrical Engineering, at the University of Zilina. His research interests include power electronics, simulations (FEM, time-domain, multilevel) and power converters optimization, design and application.

Anna KONDELOVA was born in Trstena, Slovak Republic. She graduated at Slovak Technical University in Bratislava (1983). She finished her Ph.D. study in the field of Process Control at the University of Zilina (2013). Nowadays she works at the Department of Mechatronics and Electronics, Faculty of Electrical Engineering, at the University of Zilina. Her research interests include programmable circuits, electronics, and simulations.